

3D MODELING OF LUNAR PIT WALLS FROM STEREO IMAGES. R. V. Wagner and M. S. Robinson. School of Earth and Space Exploration, Arizona State University, Tempe, AZ 85287-3603 (rvwagner@asu.edu).

Introduction: The Lunar Reconnaissance Orbiter (LRO) Narrow Angle Camera (NAC) consists of two line-scan cameras aimed side-by-side with a combined 5.7° FOV and a nominal pixel scale of 0.5 m from an altitude of 50 km [1]. To date, over 300 lunar pits have been discovered, all but three from analysis of NAC images [2], and recent measurements suggest that some may be associated with extant lava tubes [3,4]. This study builds on previous work modelling the walls and potential void spaces [5] by creating three dimensional models of the walls and mapping the extent of layering.

Methods: For four of the 16 known mare pits, LROC has acquired multiple oblique views at different slew angles, often with similar lighting, providing off-nadir stereo pairs that allow the construction of a depth map of one or both walls. We used two techniques to build models of each pit: trigonometrically solving for point position given two images, and running a network of manually-matched points through USGS ISIS software *jigsaw*, bundle-adjustment software that reports tie point positions in 3D [6].

Tie point selection: For stereo pairs with matching lighting and pixel scale, we produced an initial control network of matching points using the ISIS tool *findfeatures* [6]. The automatic match points were manually verified, and supplemented with points matched manually. When automatic matches could not be successfully generated due to lighting differences, we used only manual matches (Fig. 1). Current point spacing averages ~ 4 pixels (4-10 m), depending on density of high-contrast features, for ~ 100 -200 points per wall.

To compensate for differing pixel aspect ratios between images due to altitude and exposure time differences, all images were scaled in the down-track direction such that the pixel width and height were identical when projected on a plane perpendicular to the boresight. This correction made manual selection of match points faster and more accurate. As ISIS keeps track of scaling transformations applied to an image relative to the SPICE data, this correction does not affect

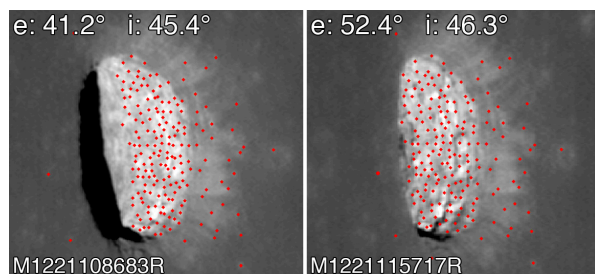


Fig. 1: Manually created tie points for the east wall of the Mare Tranquillitatis pit. The resulting model is presented in Figs. 2 and 3.

the output from *jigsaw* (verified by testing a control network built from a non-scaled stereo pair).

Trigonometric Method: Using the assumptions that the orbit tracks of two images are parallel and that the recorded spacecraft positions are exact (close to correct, given LRO's polar orbit with $>88^\circ$ inclination and <20 m positional uncertainty [7]; these assumptions give an uncertainty of <0.25 m), we treat the position of each tie point relative to an arbitrary reference point as a 2D trigonometric problem to obtain cross-track and vertical position, plus a down-track offset based on the number of lines between the tie point and reference point in each image. The resulting point cloud is re-oriented in 3D space using control points collected from NAC DTMs tied to the LOLA reference frame [8].

Jigsaw: We also produced point clouds using ISIS *jigsaw*, correcting only the camera pointing, not the position. The *jigsaw* results are very similar to the above method, with a median point offset of <1.6 m at all sites.

Results: Overhangs and Caves: The currently-measured pit walls are generally nearly vertical to slightly overhung (Fig. 2). We have identified a wall/floor contact under an overhang along the entire east wall of the Marius Hills pit (Fig. 2D), and at a single point under the SW rim of the Mare Ingenii pit (~ 15 m beyond the rim in the approximate downslope direction of the floor; further south than the Fig. 2B profile). The bottom ~ 40 m of the Mare Tranquillitatis pit (Fig. 2C; rough floor depth marked by thin orange line at bottom of figure) cannot be modelled with current images; our previous work has constrained the overhang angle on the lower east wall to $<40^\circ$ off-vertical [5], while the lower west wall has not been observed.

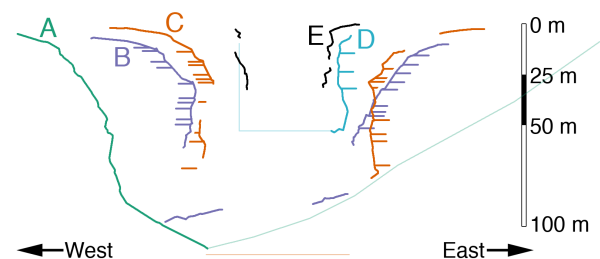


Fig. 2: East-west profiles across all four lunar pits with wall stereo images: A) Lacus Mortis pit, B) Mare Ingenii pit, C) Mare Tranquillitatis pit, D) Marius Hills pit (no coverage exists for west wall), and for comparison, E) East Twin Pit on Earth (model made with synthetic NAC images matching those used for C). Horizontal and vertical scales are the same. Horizontal lines mark measured layers (not necessarily at the position of the profile); thin lines denote approximate locations of surfaces that have not yet been modelled.

Layer thicknesses: We measured the depth of points that fell on horizontal linear reflectance changes or morphologic ridges, interpreted as boundaries between individual flow units [5, 9], at the Marius Hills, Mare Tranquillitatis, and Mare Ingenii pits. We found good correlation between layer boundary depths for the east and west walls of the Tranquillitatis pit (**Fig. 2**): All but one layer on the east wall matched up with a layer in the higher-resolution west wall images. Combining both walls, we find 11 layer boundaries in the top 60 m of Tranquillitatis pit wall and funnel (1.6-13.3 m spacing, mean = 5.8 m). Correlation is worse for the Ingenii pit, as the complete model is still in progress, but current measurements suggest at least 14 layer boundaries in the full funnel and wall (1.6-5.4 m spacing, mean=3.2 m). These may be underestimates of the actual number of layers, as limitations in resolution and lighting may hide some layer boundaries.

Verification: As a qualitative verification of the wall modeling, we produced triangle meshes from the point clouds, and rendered “synthetic NAC images” (3D modelling software Blender [10]) with matching lighting, viewing, and camera parameters to the actual NAC pit images. Comparing the synthetic images to NAC images that were not involved in the creation of the models (where available) indicates that the overall geometry is

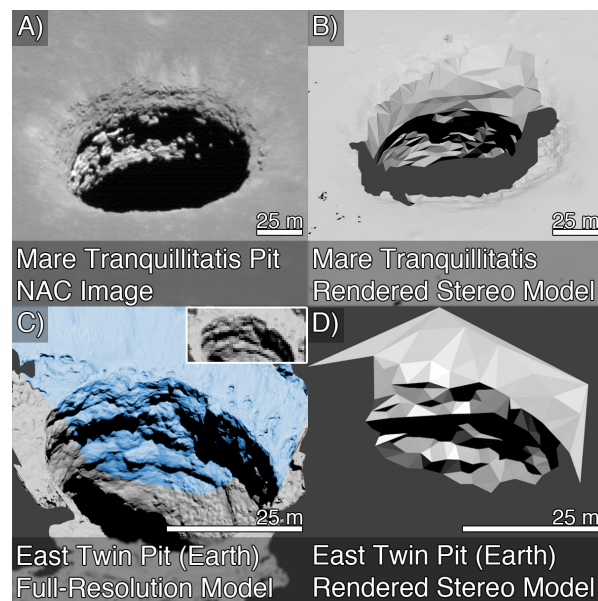


Fig. 3: A) Mare Tranquillitatis pit east wall with grazing sunlight. B) Our model, merged with a NAC DTM of the surrounding surface, rendered with matching lighting. C) Full-resolution model of the East Twin Pit in Hawai'i, with the same lighting and viewing angle. Blue region shows the approximate area visible in the images used to create the stereo model. *Inset:* Same view, at the image resolution used to produce our stereo model. D) Our model of East Twin Pit.

correct (**Fig. 3**). Smaller features such as 5-10 m wide protruding rocks are sometimes absent, but can often be restored by adding points to outline the feature.

For an additional quantitative test, we produced a model of a terrestrial pit crater using synthetic NACs of a high-resolution 3D model [5] with the same imaging parameters, including resolution, as the images we used to model the Mare Tranquillitatis pit. We aligned the low-resolution point clouds for each wall to the original model via the Iterative Closest Point algorithm, and measured the distance using the software CloudCompare [11]. The overall RMS error was 65 cm (80 cm east wall, 40 cm west wall), with no correlation between X/Y/Z position and error, indicating that this method produces dimensionally accurate models, with errors on the order of the source image pixel scale.

Conclusions: We have produced accurate 3D models of six walls of four lunar pits, and measured layer thicknesses for five of the walls. Assuming flow layers are horizontal and continuous across each pit, we found a mean layer thickness of 3-6 m.

References: [1] Robinson et al. (2010), *Space Sci. Rev.* doi: 10.1007/s11214-010-9634-2. [2] Wagner and Robinson (2014), *Icarus*, 237C, 52–60. doi: 10.1016/j.icarus.2014.04.002 [3] Chappaz et al. (2017), *Geophys. Res. Lett.*, 44, 105-112 [4] Kaku et al. (2017) *Geophys. Res. Lett.*, 44, 10,155-10,161, doi: 10.1002/2017GL074998. [5] Wagner et al. (2018), 49th LPSC, #1538. [6] Sides et al. (2017), 48th LPSC, #2739. [7] Mazarico et al. (2018), *Planet. and Space Sci.* doi:10.1016/j.pss.2017.10.004 [8] Henriksen et al. (2017), *Icarus*, 283, 122-137 doi: 10.1016/j.icarus.2016.05.012 [9] Robinson et al. (2012), *Planet. and Space Sci.*, 69, 18-27. doi: 10.1016/j.pss.2012.05.008 [10] www.blender.org [11] www.cloudcompare.org/ [12] Wagner et al. (2017), 48th LPSC, #1201. [13] Yokota et al. (2018), 49th LPSC, #1907.

Appendix A: New mare pit: We have located one new mare pit since our last publication, bringing the total known to 16 [2, 12, 13]. The inner pit is ~30×20×30 m with a large funnel, and is located in southwest Mare Tranquillitatis (4.145° N, 24.686° E). Layers are visible in both the funnel and wall (**Fig. 4**), similar to other mare pits. However, as there is currently no oblique LROC imagery of this pit, we cannot calculate layer thicknesses.

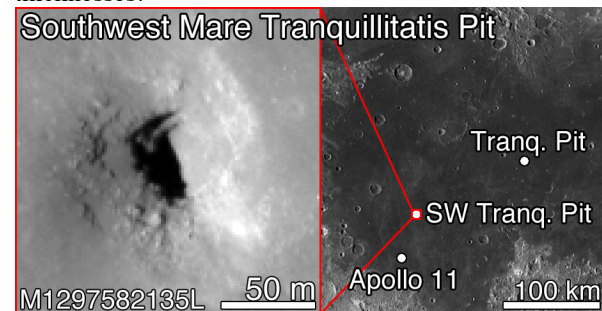


Figure 4: Newly-discovered pit in southwest Mare Tranquillitatis, showing context relative to the previously-known Mare Tranquillitatis pit.